RESEARCH ARTICLE

Macromolecular Chemistry and Physics
www.mcp-journal.de

# Synthesis and Characterization of Highly Thiolated Silk Fibroin

*Jeremy M. Talusig and Amanda R. Murphy**

**Covalent attachment of thiols to the tyrosine residues of silk fibroin is accomplished with a high degree of functionalization through the reaction of a pyridyldithiol-containing N-hydroxysuccinimidal-ester and an amino-tyrosine silk intermediate. The extent of thiol modification is characterized by $^1$H NMR and UV–vis spectroscopy. Further modification of the thiol groups is probed by reacting with an iodoacetamide-containing small molecule resulting in a novel fluorescent silk derivative. Last, the ability of the thiolated silk to form hydrogels in situ is investigated.**

## 1. Introduction

The study of silk has gained traction in recent years for its wide-ranging use in biomedical applications.[1] The popularity of silk can be attributed to the fact that it is easily processable, biocompatible, biodegradable, and has robust mechanical properties.[2,3] The most commonly used type of silk is that produced by the *Bombyx mori* silkworm, which is readily available in large quantities. Methods have been established to extract the silk protein from cocoons and reprocess it into versatile structures such as fibers, hydrogels, films, micro/nanoparticles, etc.[1,4–9] Chemical modification methods for silk fibroin have also become highly sought after to tailor the material for use in drug delivery, tissue engineering, bioelectronics, and more.[10–12] The majority of amino acids in silk are inert, where glycine and alanine combined make up 76.2 mol% of the protein. However, a small fraction of the amino acids in silk are reactive and available for modification including serine (12.1 mol%), threonine (0.9 mol%), tyrosine (5.3 mol%), aspartic acid (0.5 mol%), glutamic acid (0.6 mol%) and lysine (0.2 mol%).[13] To date, the most highly utilized methods to create covalent linkages to native functional groups within silk fibroin are carbodiimide coupling with the aspartic/glutamic acid or lysine residues and diazonium couplings to modify tyrosine.[10–12]

While the list of covalent modifications available for silk continues to grow, chemistry involving thiols has not been widely explored. Thiols are important bridging structures in nature as proven by their existence in polysaccharides, proteins, and natural products. Their relatively low pKa and high nucleophilicity render thiols reactive in physiological conditions making them popular for site-selective protein labeling.[14] The ability of thiols to form reversible disulfide bonds has also been utilized to create self-healing hydrogels, redox-responsive hydrogels, mucosal adhesives, and drug-delivery vehicles from other synthetic and natural polymer systems.[15–19] However, native cysteines are present in extremely low concentrations in silk fibroin, making up less than 0.1 mol% of the amino acid content. Previous reports are sparse on increasing the thiol-content of silk through chemical modification. Cysteine[20] and glutathione[21,22] have been reacted with the aspartic and glutamic acid residues of silk by *N*-ethyl-*N*′-(3-(dimethylamino)propyl)carbodiimide / N-hydroxysuccinimide (EDC-NHS) coupling. However, aspartic and glutamic acid combined make up a mere 1.5 mol% of silk, therefore the extent of modification by carbodiimide coupling is limited. Silk has also been functionalized with sulfhydryl groups by targeting the lysine residues of silk with 2-iminothiolane (Traut's reagent).[23] In this case, the extent of modification is even lower as silk only contains 0.2 mol% lysine.

The scarcity of methods available for the installation of thiols into silk with a high degree of functionalization warrants further research. Here, a strategy is outlined to incorporate sulfhydryl groups into silk by targeting the more abundant tyrosine residues (5 mol%). The ability to conjugate small molecules to the thiol groups and form disulfide crosslinked hydrogels is also demonstrated.

## 2. Results and Discussion

### 2.1. Synthesis and Characterization of SPDP-silk

A two-step method previously reported by our group was first employed to increase the number of nucleophilic reaction sites in silk through the addition of an amine to the tyrosine residues (**Scheme 1**).[24] Silk contains an unusually high amount of tyrosine and thus this reaction sequence can provide up to 277 new nucleophilic reactive sites per silk molecule (5 mol%). Here, methods are described to further functionalize these new reactive sites to append thiol-containing molecules onto each of the tyrosine residues (Scheme 1).

A related strategy has been reported previously, where the authors attempted to increase the number of nucleophilic amine groups in silk by reacting tyrosine with a diazonium salt

J. M. Talusig, A. R. Murphy
Department of Chemistry
Western Washington University
516 High St., Bellingham, WA 98225-9150, USA
E-mail: amanda.murphy@wwu.edu

The ORCID identification number(s) for the author(s) of this article can be found under https://doi.org/10.1002/macp.202300340

**DOI: 10.1002/macp.202300340**

 

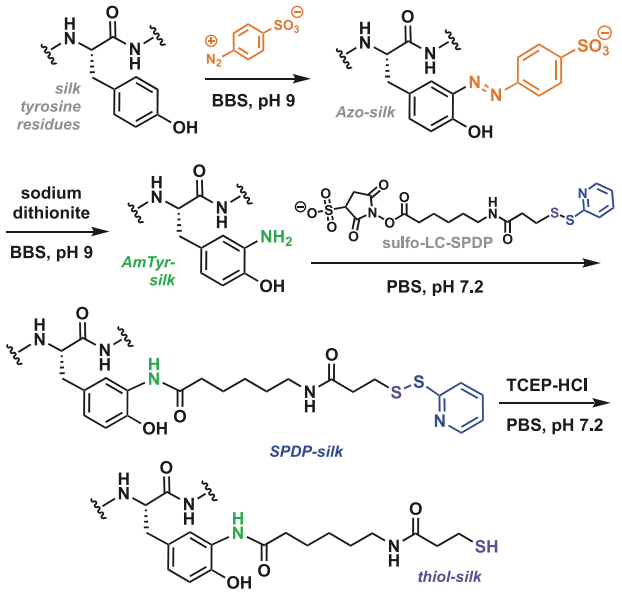


**Scheme 1.** Synthesis scheme for converting the tyrosine residues in silk to thiol-silk.

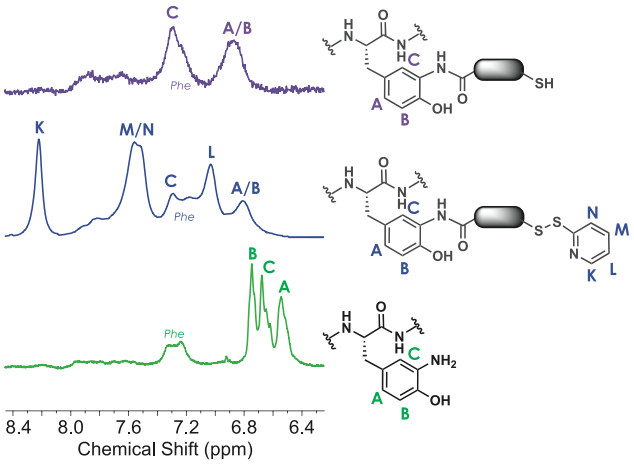


**Figure 1.** The aromatic region of the $^{1}$H NMR spectra of AmTyr-silk (green), SPDP-silk (blue), and thiol-silk (purple) confirm tyrosine modification. Full spectra are provided in Figure S1, Supporting Information.

containing a primary amine, followed by NHS modification to add thiol-containing groups.[25] However, diazonium reactions work poorly with electron-rich anilines leading to a low conversion.[26] The authors reported that they were only able to achieve a 1.9:1 molar ratio between the thiol-containing molecule and silk fibroin,[25] leaving significant room for improvement.

In the method reported here, the diazonium coupling reaction utilized an electron-poor aniline (sulfanilic acid) to quantitatively install azo groups on all of the tyrosine residues in silk (Scheme 1). Sodium dithionite was then used to reduce the azo bonds, resulting in a new primary amine ortho to the hydroxyl group on tyrosine, hereafter referred to as amino-tyrosine (AmTyr).[24] To avoid oxidation and degradation of the electron-rich AmTyr ring, the AmTyr-silk was used for further reactions within 1 day. We have previously demonstrated that AmTyr-silk could be amidated using carboxylic acid or NHS-ester derivatives.[24] Therefore, reactions with different electrophilic reagents containing a thiol or disulfide were explored (Scheme S1, Supporting Information). Initial experiments used Traut's reagent (2-iminothiolane hydrochloride), but poor conversions were obtained. The heterobifunctional crosslinker succinimidyl 3-(2-pyridyldithio) propionate (SPDP) was more successful. However, because SPDP is not water-soluble and must be dissolved in dimethyl sulfoxide prior to reaction, solubility, and purification became problematic with larger scale reactions. For this reason, sulfosuccinimidyl-6-(3′-(2-pyridyldithio)propionamido)hexanoate (sulfo-LC-SPDP) was utilized instead due to its high solubility in aqueous buffers (Scheme 1). To carry out the modification reaction, sulfo-LC-SPDP (3 equiv. relative to tyrosine) was dissolved in AmTyr-silk in PBS and left to react for 1 h at rt, and then purified using a disposable size exclusion column (hereafter referred to as SPDP-silk).

The modifications were confirmed using $^{1}$H NMR (full spectra are given in Figure S1, Supporting Information). Obvious changes were observed in the aromatic region of SPDP-silk as compared to the AmTyr-silk precursor (**Figure 1**). Four peaks appear in SPDP-silk from the newly installed pyridyldithiol group. The characteristic downfield peak at 8.2 ppm can be attributed to the proton next to the nitrogen on the pyridine ring (K). The remaining pyridine protons, M/N and L were assigned to the peaks at 7.6 and 7.0 ppm, respectively, using predictions from MestReNova NMR software. The chemical shifts of the tyrosine aromatic protons were also consistent with similar derivatives previously reported.[24] Protons A and B are assigned to the broad peak at 6.8 ppm and proton C was shifted downfield to 7.3 ppm. Importantly, no evidence of peaks corresponding to unreacted AmTyr-silk was found suggesting complete modification of all the tyrosine residues. Changes to the methylene region of the AmTyr-silk spectrum further corroborated the attachment of sulfo-LC-SPDP (Figure S1, Supporting Information). In the 2.5–3.5 ppm region of SPDP-silk, new peaks were observed corresponding to the methylene protons of the sulfo-LC-SPDP linker.

### 2.2. Reduction of SPDP-Silk to Form Thiol-Silk

Once silk was enriched with disulfides from the attachment of sulfo-LC-SPDP to all of the amino-tyrosine rings, reduction with tris(2-carboxyethyl)phosphine (TCEP) was carried out to generate free thiols (Scheme 1). TCEP (3 equiv. relative to tyrosine) was dissolved in ≈1% SPDP-silk in PBS and allowed to react at rt for 10–15 min. To confirm that the reduction was occurring, a $^{1}$H NMR spectrum was taken of the mixture containing SPDP-silk and TCEP. As shown in Figure S2, Supporting Information, the original pyridine peaks in SPDP-silk are absent, and sharp peaks belonging to the cleaved small molecule by-product, pyridine-2-thione (P2T), can be clearly observed. Four resonances at 7.9, 7.7, 7.6, and 7.1 ppm were assigned to the four protons on P2T. In addition, peaks corresponding to oxidized and reduced forms of TCEP were present. By the end of the reaction, the solution appeared cloudy perhaps due to the P2T by-product. For purification, dialysis and size exclusion columns were able to remove

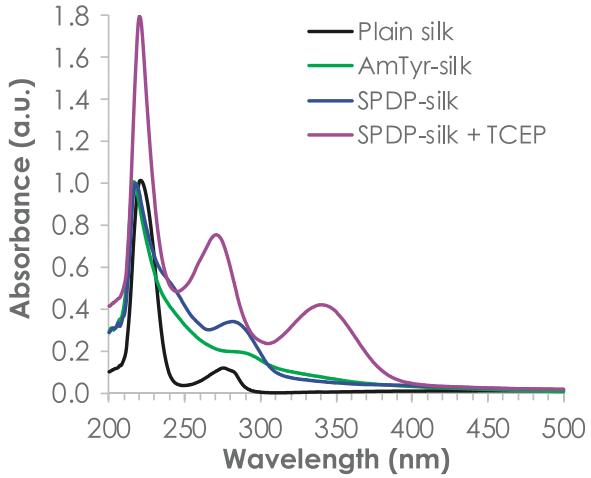


**Figure 2.** UV/vis spectra of the silk derivatives in PBS buffer. The plain, AmTyr, and SPDP-silk samples were normalized to the peak at ≈220 nm. The pink spectrum was generated from the same SPDP-silk sample noted in blue after incubation with TCEP for ≈15 min.

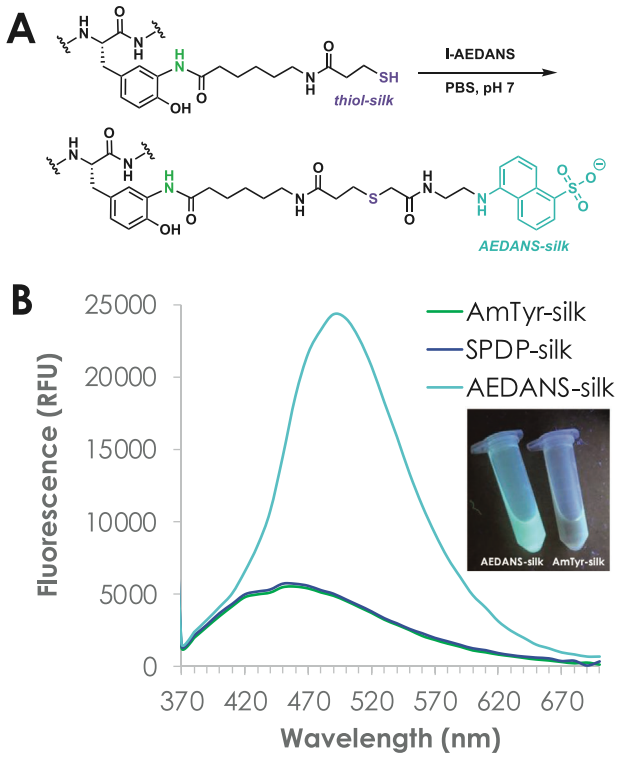


**Figure 3.** A) Reaction scheme to attach AEDANS to thiol-silk. B) Fluorescence emission spectra of the noted silk derivatives in PBS when excited at 336 nm. The inset photo compares the visible emission from AEDANS-silk versus AmTyr-silk under a long-wave UV light.

the P2T, but insufficient at removing the excess TCEP. However, washing with PBS in a centrifugal concentrator was effective at removing all of the impurities. Following purification, the NMR spectrum of thiol-silk shows only two broad peaks belonging to the remaining tyrosine protons of thiol-silk (Figure 1). The peaks assigned to the tyrosine protons A, B, and C of thiol-silk were found at similar chemical shifts to that seen in SPDP-silk since the disulfide reduction does not directly impact the tyrosine ring. Most notably, peaks belonging to the pyridine protons (KLMN) were absent signifying complete cleavage to produce a free thiol moiety.

The P2T also has a unique absorbance at 343 nm, therefore UV/vis could be utilized to monitor the cleavage reaction (**Figure 2**). For reference, the spectrum of unmodified silk is given in black showing the original tyrosine absorbance at 273 nm. The addition of the amino group to the ring shifts the tyrosine peak to 290 nm (Figure 2, green). An increase in absorption was found after reaction with LC-SPDP, but peak positions did not significantly change (Figure 2, blue). To monitor the disulfide cleavage reaction, a concentrated solution of TCEP (3 equiv. relative to tyrosine) was added directly to the cuvette containing SPDP-silk, and the absorbance was re-recorded after 10–15 min (Figure 2, pink). New peaks at 266 and 343 nm appeared corresponding to the cleaved product P2T, further confirming its presence. The spectrum was unchanged after adding more TCEP indicating the reaction was complete. The extent of SPDP modification was calculated from the spectra following the manufacturer's protocol (ThermoFisher #21650), where the molar ratio of P2T to silk was estimated to be ≈140:1. However, this spectroscopic method requires a known molarity of the silk solution, which is difficult to measure accurately as the silk protein is large and known to break down during the extraction process producing a distribution of molecular weights.[27] While the UV spectra can only provide an estimate of the extent of the reaction, it does corroborate the NMR data suggesting a high level of modification of the 277 tyrosine residues in silk.

### 2.3. Conjugation of a Fluorescent Iodoacetamide to Thiol-Silk

With a reproducible way in hand to incorporate free sulfhydryl groups into silk, the fluorescent molecule 5-(((2-iodoacetyl)amino)ethyl)amino)naphthalene-1-sulfonic acid (IAEDANS) was used to probe the reactivity of the thiols. In buffers above pH 4, IAEDANS is highly soluble in water and undergoes selective reaction with thiols to produce a thioether-coupled product. Additionally, when excited at 336 nm, the AEDANS moiety has a fluorescent emission at 490 nm, which made it attractive to verify its conjugation to thiol-silk.

Once thiol-silk was produced, 7.5 equiv. (relative to tyrosine) of IAEDANS was dissolved in the silk solution and the reaction was incubated at rt for ≈3 h in the dark (**Figure 3**A). Following purification via size-exclusion, fluorescence spectra were collected for all silk derivatives. As shown in Figure 3B, when excited at 336 nm, both AmTyr-silk and SPDP-silk had a low, broad emission centered around 460 nm. This emission has been previously attributed to the intrinsic fluorescence of aggregated tyrosine and tryptophan residues in silk.[28,29] In contrast, the AEDANS-silk displayed a strong, distinct emission at 490 nm corresponding to the newly installed naphthalene chromophore, confirming the presence of the AEDANS moiety.

The AEDANS group contains a polycyclic aromatic system, thus modifications to the thiol-silk could also be tracked by evaluating the aromatic region of the AEDANS-silk proton NMR

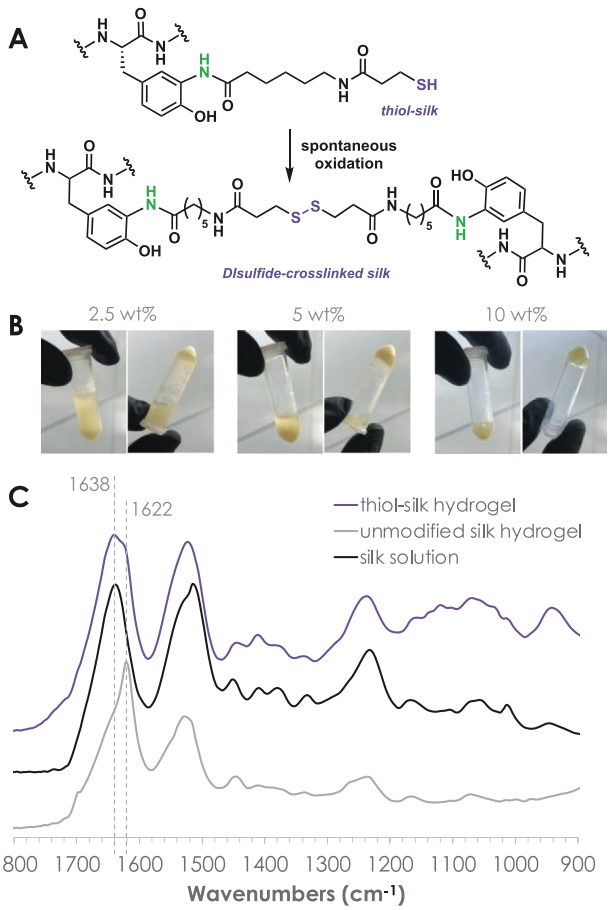


**Figure 4.** A) Depiction of the proposed oxidation of thiol-silk to form disulfide crosslinks. B) Photos of 2.5, 5, and 10 wt% thiol-silk hydrogels. C) ATR-FTIR spectra of lyophilized samples of silk solution, an unmodified silk hydrogel, and a thiol-silk hydrogel (both gels are 10 wt% silk).

(Figure S3, Supporting Information). New resonances appear in this region, which can be assigned to each of the aromatic naphthalene protons. The tyrosine protons remain where they were found for thiol-silk as expected. Additional peaks were also found in the 2–3.5 ppm region of the AEDANS-silk spectrum corresponding to the methylene protons in the IAEDANS linker. Examining both the proton NMR and fluorescence spectra of AEDANS-silk, the successful conjugation of IAEDANS to the thiol-silk could be confirmed.

### 2.4. In Situ Gelation and Characterization of Thiol-Silk Hydrogels

Unmodified silk fibroin in solution will naturally increase in $\beta$-sheet content over time, eventually forming a hydrogel. This gelation process usually takes weeks at room temperature and neutral pH, but can be accelerated by adjusting pH, adding organic co-solvents, applying physical stimuli, or adding chemical crosslinking agents.[30] Here, it was envisioned that chemical crosslinks via disulfide bonds between the newly installed thiol groups would be enough to rigidify the structure of silk fibroin to form a hydrogel (**Figure 4**A). Therefore, varying concentrations of thiol-silk were investigated for their gelling capabilities. Briefly, thiol-silk solutions were concentrated in a centrifugal concentrator to 10 wt% and then diluted with PBS to give final concentrations of ≈2.5, 5, and 10 wt% silk. These thiol-silk solutions were left undisturbed at rt and gelation was monitored over time (Figure 4B). As expected, the higher concentrations of silk were able to completely gel in a shorter amount of time. For all concentrations of thiol-silk, the early stage of gelation (the solution-gel transition) was observed within 24 h indicated by a change of clarity of the solution from clear to cloudy. In 3–4 days, the 10 wt% thiol-silk showed complete gelation by tube inversion. For 5 wt% thiol-silk solutions, most of the silk appeared gelled by day 12 at rt, but samples contained a small amount of water that did not stay encapsulated in the gel. The 2.5 wt% thiol-silk showed some gelling/precipitation by inversion, but did not form a cohesive gel and most of the water was excluded from the solid. Photos of each type of gel before and after inversion are provided in Figure 4B. For comparison, solutions of unmodified silk at the same concentrations were also monitored over the same time period, but no changes in solution clarity or gelation were observed.

Since the 10 wt% thiol-silk was most successful at forming a hydrogel, FTIR was further employed to determine if the gelation was due to natural $\beta$-sheet formation (physical crosslinks) or disulfide bond formation (chemical crosslinks). The secondary structure of silk can be determined by examining the amide I (C═O stretch), amide II (N-H bend), and amide III band (C-N bend).[31] It is very common to see the carbonyl peak shift from higher wavenumbers to lower wavenumbers when silk is physically or chemically crosslinked demonstrating a conformational change of the silk from a random coil to a crystalline beta sheet arrangement. ATR-FTIR spectra were recorded for a dried 10 wt% thiol-silk hydrogel, a dried unmodified silk hydrogel formed through spontaneous crystallization of silk solution (took several weeks at rt to form), and lyophilized silk solution (Figure 4B). For the unmodified silk hydrogel, the amide carbonyl stretch was observed at 1620 $cm^{-1}$, consistent with literature values for silk structures that contain a high amount of $\beta$-sheet content.[31] In contrast, the amide stretch of the lyophilized silk solution was found at 1637 $cm^{-1}$, which is consistent with a less ordered, random coil structure expected for the soluble form of the protein.[31] As noted in Figure 4B, the amide peak for the thiol-silk gel was centered at 1638 $cm^{-1}$ with only a slight shoulder at lower wavenumbers. This indicated that most of the silk within the gel remained in a random coil state. Therefore, it could be determined that $\beta$-sheet formation was not the major driving factor for gelation of the thiol-silk. Considering that the 10 wt% thiol-silk solution formed a hydrogel much more rapidly than unmodified silk (days versus weeks) and the resulting gel exhibited low $\beta$-sheet content, we can conclude that the newly-installed thiols are playing an important role in the gelation mechanism. Further work is currently underway to fully evaluate the parameters needed for robust gelation, the potential reversibility of the gelation and to characterize the rheological and mechanical properties of these materials.

## 3. Conclusions

The lack of native cysteine residues in silk has limited the use of versatile thiol chemistries to produce functional silk derivatives. Here, we demonstrate a method to append a linker containing a

thiol group to the large number of tyrosine residues present in silk fibroin. By $^1$H NMR, the reaction sequence is quantitative at each step, resulting in the highest level of thiol incorporation reported to date for *B. mori* silk. The ability to further modify the sulfhydryl groups was probed using a thiol-specific iodoacetamide, producing a novel fluorescent silk derivative. Preliminary investigations into the ability of the thiol-silk to form hydrogels in situ were also carried out, and gelation via disulfide bond formation was confirmed using FTIR. Overall, the installation of thiols through an amino-tyrosine intermediate is a promising advancement toward new thiol-silk-based biomaterials and drug delivery systems.

## 4. Experimental Section

*Instrumentation*: NMR of silk solutions was performed on a Bruker Avance III 500 MHz spectrometer. FTIR of dried silk gels were recorded on a Thermo Nicolet 6700 FTIR using an attenuated total reflectance (ATR) crystal. UV–vis spectra of silk solutions were collected using a Jasco UV-vis-NIR spectrometer and fluorescence spectra were collected on a BioTek Synergy H1 model plate reader.

*Silk Molarity Calculations*: Silk is known to degrade during the purification and solubilization process leading to a dispersity in molecular weight that makes the reagent calculations imprecise.[27] To estimate the amounts of reagents needed for each reaction, the molar ratios reported below were calculated assuming the full molecular weight of silk (391 kDa) and the fact that silk contains 5.3 mol% tyrosine (277 tyr residues per protein). The concentration (mg mL$^{-1}$) of silk solutions was determined by drying aliquots of the solution in an oven at 60 °C for at least 1 h and weighing the residual protein.

*Preparation of AmTyr-Silk Solution*: AmTyr-silk solution was produced as described previously.[24] Briefly, aqueous solutions of *B. mori* silk in borate-buffered saline were prepared. A diazonium coupling reaction was then carried out to install azo groups on the tyrosine residues in silk. This reaction was repeated twice to ensure complete modification. The azo-silk derivatives were further reacted with sodium dithionite to reduce the azo bonds resulting in a primary amine ortho to the hydroxyl group on tyrosine. The reaction solution was purified and exchanged into PBS using disposable size exclusion columns.

*Sulfo-SPDP Modification of AmTyr-Silk*: Immediately after the reduction and purification of AmTyr-silk, 32.0 mg (0.06 mmol; 3 equiv. relative to tyrosine) of sulfo-LC-SPDP (Campbell Science) was dissolved in 1.0 mL of ≈3% w/v AmTyr-silk in PBS (all PBS used throughout contained: 0.1 M sodium phosphate, 0.15 M NaCl, pH 7.2), and allowed to react for 1 h at rt with rocking. The reaction solution was passed through a size exclusion column (Cytiva, NAP-10) pre-equilibrated with PBS for purification. For NMR, 0.5 mL of purified SPDP-silk was exchanged into $D_2O$ using a size exclusion column (Cytiva, NAP-5). $^1$H NMR (500 MHz, $D_2O$): $\delta$ 8.2 (m, 1H), 8.1–7.4 (m, 3H), 7.4–6.9 (m, 3H), 6.8 (m, 1H), 4.5 (m, 3H), 4.3 (m, 6H), 4.1–3.8 (m, 21H), 3.3–2.7 (m, 6H), 2.7–2.2 (m, 3H), 1.6–1.5 (m, 3H), 1.5–1.0 (m, 21H), 1.0–0.7 (m, 3H).

*Reduction of SPDP-Silk*: Immediately after purification of SPDP-silk, 11.6 mg (0.04 mmol; 3 equiv. relative to tyrosine) of TCEP·HCl was added to 1.0 mL of ≈2% w/v SPDP-silk in PBS, vortexed to dissolve, then left to react for 10–15 min. For purification, the reaction mixture was loaded into a centrifugal concentrator (Vivaspin 6; MWCO 10 000) and spun at 4000 RPM and 4 °C for ≈45 min or until the volume was reduced by ≈75%. Next, 1 mL of PBS was added, and the solution was spun again until the volume was reduced by ≈75%. The final solution was used as is or diluted with PBS to the desired concentration. For NMR, 0.5 mL of the purified thiol-silk was exchanged into $D_2O$ using a size exclusion column (Cytiva, NAP-5). The resulting thiol-silk should be used immediately. Alternatively, more TCEP can be added to the PBS-buffered thiol-silk solution to prevent premature oxidation and should be stored under refrigeration. Thiol-silk $^1$H NMR (500 MHz, $D_2O$): $\delta$ 8.0–7.5 (m, 1H), 7.3 (m, 1H), 6.9 (m, 1H), 4.5 (m, 2H), 4.3 (m, 5H), 4.0–3.8 (m, 19H), 3.1 (m, 2H), 3.0–2.6 (m, 2H), 2.5 (m, 2H), 1.8–1.5 (m, 2H), 1.5–1.1 (m, 21H), 1.0–0.7 (m, 3H).

*Attachment of I-AEDANS to SPDP-Silk*: To covalently attach IAEDANS to thiol-silk, 28.6 mg (0.06 mmol, 7.5 equiv. relative to tyrosine) of IAEDANS was dissolved in 1 mL of ≈1 wt% thiol-silk in PBS and left for 3 h at rt. To keep the reaction from degrading in light, the reaction vessel was covered in foil. Afterward, the reaction solution was passed through a NAP-10 column (Cytiva) pre-equilibrated with PBS. Alternatively, the solutions could be dialyzed against PBS for 2 days, changing the buffer twice. Dialyzed samples were concentrated as needed using a centrifugal concentrator (Vivaspin 6; MWCO 10 000). NMR samples were exchanged into $D_2O$ using a NAP-5 column. AEDAN-Silk $^1$H NMR (500 MHz, $D_2O$): $\delta$ 8.2–7.9 (m, 2H), 7.6–7.0 (m, 4H), 6.9 (m, 2H), 6.6 (m, 1H), 4.5 (m, 2H), 4.3 (m, 4H), 4.1–3.7 (m, 12H), 3.5 (m, 1H), 3.3–2.7 (m, 6H), 2.7–2.4 (m, 2H), 2.3 (m, 3H), 2.1 (m, 1H), 1.7–1.5 (m, 2H), 1.4–1.0 (m, 13H), 1.0–0.7 (m, 3H).

*Gelation of Thiol-Silk*: To acquire different concentrations of the thiol-silk for gelation studies, the purified solutions were placed into a centrifugal concentrator (Vivaspin 6; MWCO 10 000) and spun at 4000 RPM and 4 °C until the solution was >10% w/v. The solution was then diluted to 2.5, 5, and 10% w/v using PBS. The thiol-silk samples were then allowed to sit at rt to observe gelation or any changes in viscosity over time.

## Supporting Information

Supporting Information is available from the Wiley Online Library or from the author.

## Acknowledgements

This work was supported by the National Science Foundation under grant no. DMR-1807878 and a Henry Dreyfus Teacher Scholar Award (A.R.M.). The authors are grateful for assistance from John Antos, Hla Win-Piazza, Mark Lorenz, and Kyle Mikkelsen with analytical techniques and instrumentation. The NMR data acquisition on the 500 MHz NMR spectrometer was made possible through an NSF-MRI award (award no. 1532269).

## Conflict of Interest

The authors declare no conflict of interest.

## Data Availability Statement

The data that support the findings of this study are available from the corresponding author upon reasonable request.

## Keywords

protein modification, silk, thiol, tyrosine

Received: September 19, 2023
Revised: October 25, 2023
Published online:

[1] C. Holland, K. Numata, J. Rnjak-Kovacina, F. P. Seib, *Adv. Healthcare Mater.* **2019**, *8*, 1800465.
[2] Y. Wang, H.-J. Kim, G. Vunjak-Novakovic, D. L. Kaplan, *Biomaterials* **2006**, *27*, 6064.

[3] G. H. Altman, F. Diaz, C. Jakuba, T. Calabro, R. L. Horan, J. Chen, H. Lu, J. Richmond, D. L. Kaplan, *Biomaterials* **2003**, *24*, 401.
[4] L.-D. Koh, J. Yeo, Y. Y. Lee, Q. Ong, M. Han, B. C.-K. Tee, *Mater. Sci. Eng., C* **2018**, *86*, 151.
[5] M. Ru, A. M. Hai, L. Wang, S. Yan, Q. Zhang, *Int. J. Biol. Macromol.* **2023**, *224*, 422.
[6] R. D. Abbott, E. P. Kimmerling, D. M. Cairns, D. L. Kaplan, *ACS Appl. Mater. Interfaces* **2016**, *8*, 21861.
[7] B. Yu, Y. Li, Y. Lin, Y. Zhu, T. Hao, Y. Wu, Z. Sun, X. Yang, H. Xu, *Front. Pharmacol.* **2023**, *13*, 1071868.
[8] T. Yucel, M. L. Lovett, D. L. Kaplan, *J. Controlled Release* **2014**, *190*, 381.
[9] B. Zhu, H. Wang, W. R. Leow, Y. Cai, X. J. Loh, M.-Y. Han, X. Chen, *Adv. Mater.* **2015**, *28*, 4250.
[10] A. R. Murphy, D. L. Kaplan, *J. Mater. Chem.* **2009**, *19*, 6443.
[11] J. K. Sahoo, O. Hasturk, T. Falcucci, D. L. Kaplan, *Nat. Rev. Chem.* **2023**, *7*, 302.
[12] S. A. L. Matthew, F. P. Seib, *ACS Biomater. Sci. Eng.* **2023**, https://doi.org/10.1021/acsbiomaterials.2c01116.
[13] C.-Z. Zhou, F. Confalonieri, M. Jacquet, R. Perasso, Z.-G. Li, J. Janin, *Proteins* **2001**, *44*, 119.
[14] P. Ochtrop, C. P. R. Hackenberger, *Curr. Opin. Chem. Biol.* **2020**, *58*, 28.
[15] V. Puri, A. Sharma, P. Kumar, I. Singh, *Polymers* **2020**, *12*, 1803.
[16] S. Summonte, G. F. Racaniello, A. Lopedota, N. Denora, A. Bernkop-Schnürch, A. Bernkop-Schnürch, *J. Controlled Release* **2021**, *330*, 470.
[17] J. Su, *Gels* **2018**, *4*, 72.
[18] I. Altinbasak, S. Kocak, R. Sanyal, A. Sanyal, *Biomacromolecules* **2022**, *23*, 3525.
[19] R. K. Boz, D. Aydin, S. Kocak, B. Golba, R. Sanyal, A. Sanyal, *Bioconjugate Chem.* **2022**, *33*, 839.
[20] S. Das, B. B. Dhar, *RSC Adv.* **2014**, *4*, 46285.
[21] X. Zhang, H. Bao, C. Donley, J. Liang, S. Yang, S. Xu, *BMC Chem.* **2019**, *13*, 62.
[22] X. Zhang, J. Liang, Z. Chen, C. Donley, X. Zhang, G. Cheng, *Processes* **2020**, *8*, 498.
[23] C. Laomeephol, H. Ferreira, S. Yodmuang, R. L. Reis, S. Damrongsakkul, N. M. Neves, *Biomolecules* **2020**, *10*, 466.
[24] K. G. Hausken, R. L. Frevol, K. P. Dowdle, A. N. Young, J. M. Talusig, C. C. Holbrook, B. K. Rubin, A. R. Murphy, *Macromol. Chem. Phys.* **2022**, *223*, 2200119.
[25] A. R. D. Reeves, K. L. Spiller, D. O. Freytes, G. Vunjak-Novakovic, D. L. Kaplan, *Biomaterials* **2015**, *73*, 272.
[26] A. R. Murphy, P. S. John, D. L. Kaplan, *Biomaterials* **2008**, *29*, 2829.
[27] L. S. Wray, X. Hu, J. Gallego, I. Georgakoudi, F. G. Omenetto, D. Schmidt, D. L. Kaplan, *J. Biomed. Mater. Res., Part B* **2011**, *99*, 89.
[28] I. Georgakoudi, I. Tsai, C. Greiner, C. Wong, J. Defelice, D. Kaplan, *Opt. Express* **2007**, *15*, 1043.
[29] O. K. Gasymov, C. Botta, L. Ragona, A. J. Guliyeva, H. Molinari, *Macromol. Chem. Phys.* **2019**, *220*, 1800460.
[30] H. Zheng, B. Zuo, *J. Mater. Chem. B* **2020**, *9*, 1238.
[31] X. Hu, D. Kaplan, P. Cebe, *Macromolecules* **2006**, *39*, 6161.

WILEY-VCH

Supporting Information

# Synthesis and Characterization of Highly Thiolated Silk Fibroin

*Jeremy M. Talusig and Amanda R. Murphy**

Department of Chemistry, Western Washington University, 516 High St., Bellingham, WA 98225-9150, USA

*Corresponding Author: amanda.murphy@wwu.edu

**Scheme S1.** Attempted reactions of AmTyr-silk with Traut's reagent and SPDP.

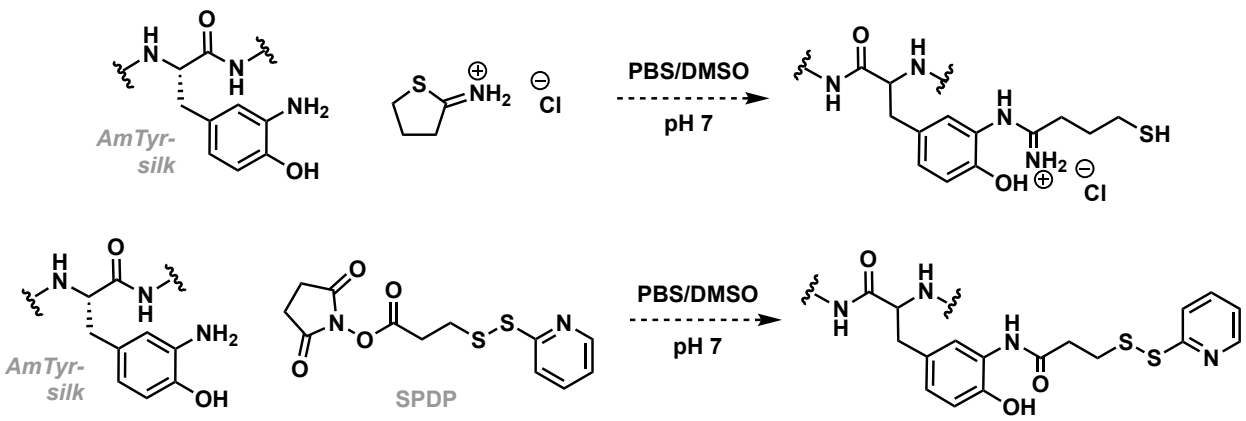


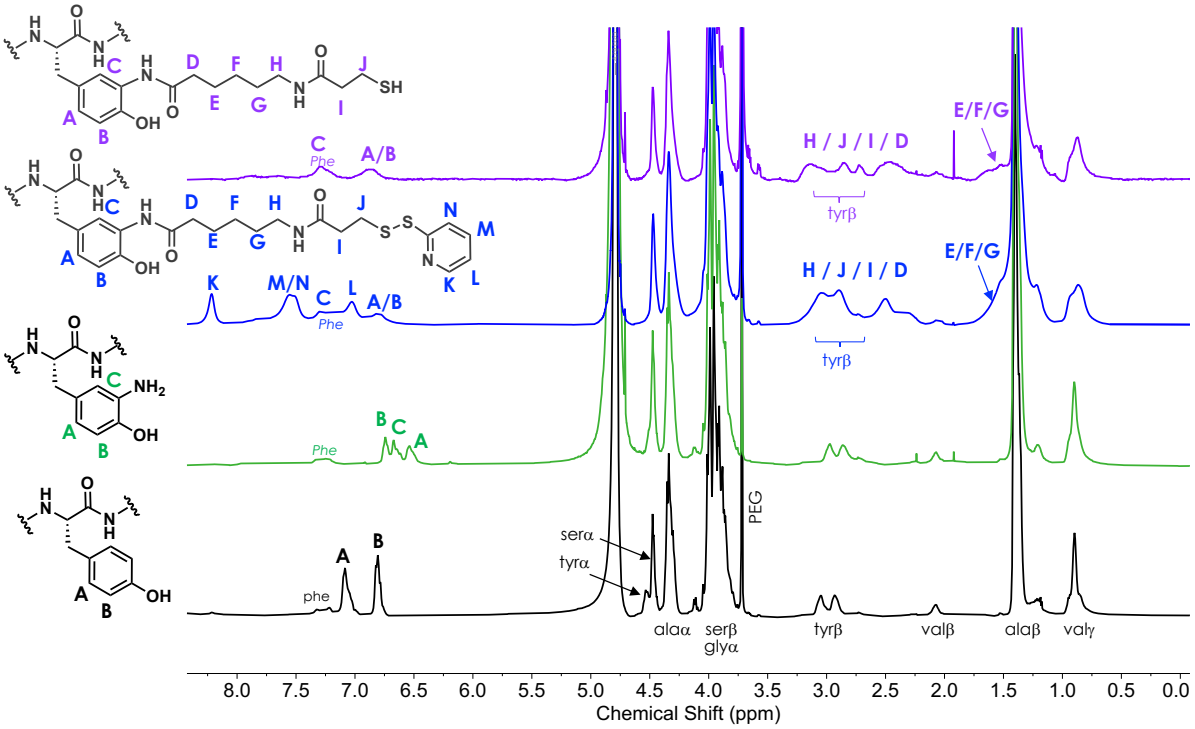


**Figure S1.** Full $^{1}$H NMR spectra with peak assignments for plain silk (black), AmTyr-silk (green), SPDP-silk (blue) and thiol-silk (purple). Amino acid resonances that are consistent across all samples are labeled at the bottom. Samples are ~0.5-1 wt% silk in $D_2O$.

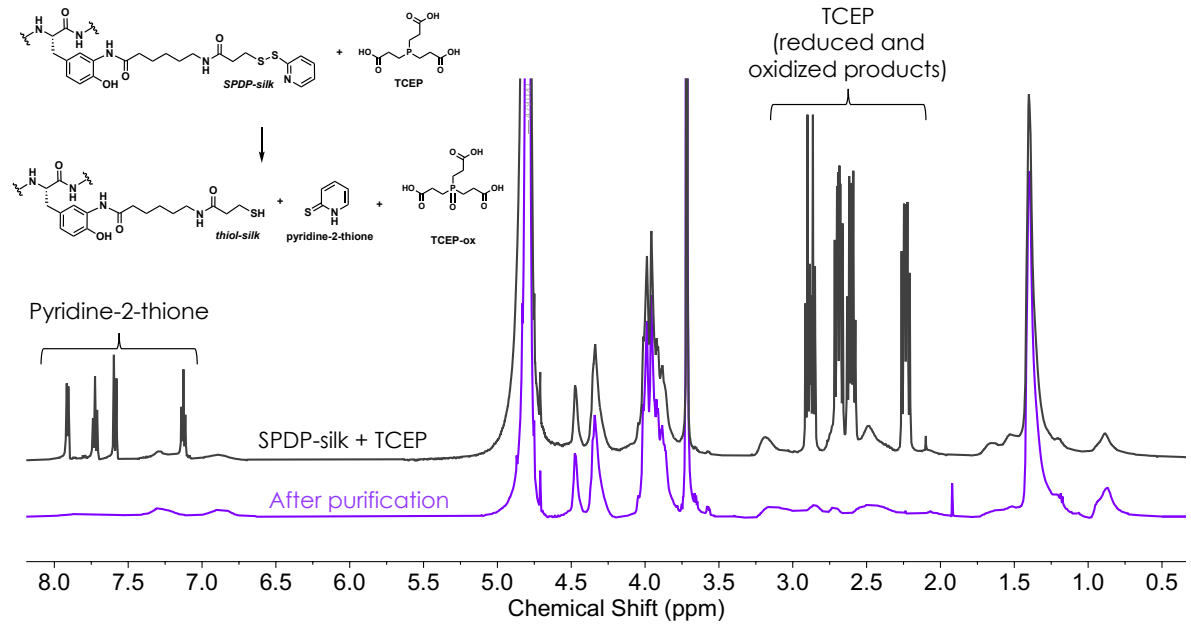


**Figure S2.** $^{1}$H NMR spectra of thiol-silk before and after purification. The black spectrum was taken of SPDP-silk 15 min after adding TCEP. Peaks for reduced and oxidized TCEP, the pyridine-2-thione by-product and thiol-silk are observed. After purification, the peaks for TCEP and pyridine-2-thione are removed.

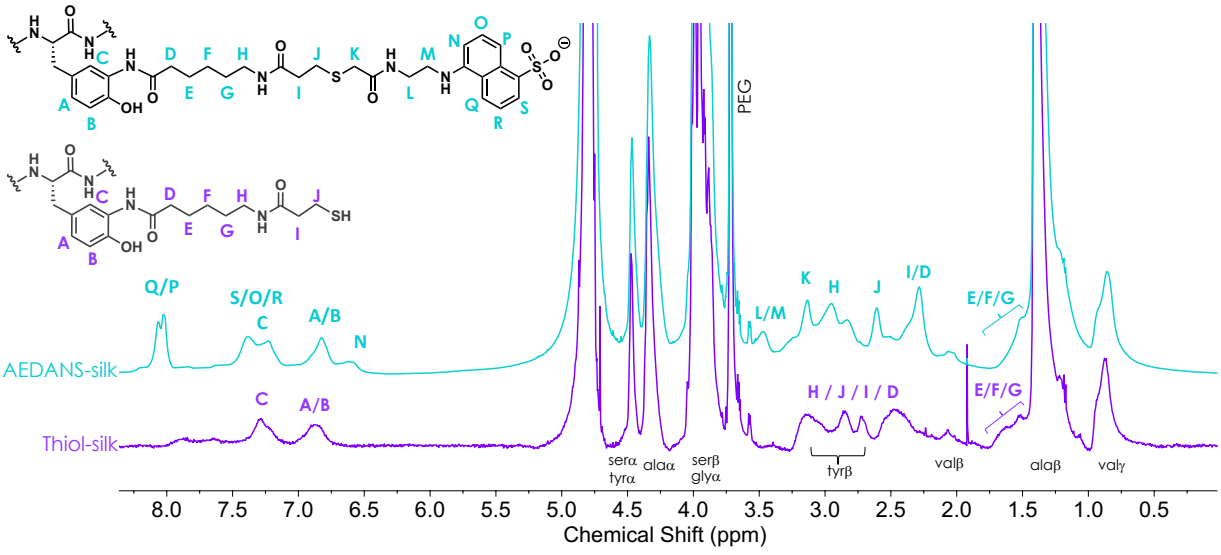


**Figure S3.** $^{1}$H NMR spectra of thiol-silk before and after reaction with IAEDANS. Samples are ~0.5 wt% silk in $D_2O$.